Ground response during offshore pile driving in a sandy slope

Lamens, Pascale; Askarinejad, Amin; Sluijsmans, Robbin W.; Feddema, Antoine

Citation (APA)
Lamens, P., Askarinejad, A., Sluijsmans, R. W., & Feddema, A. (2020). Ground response during offshore pile driving in a sandy slope. *Geotechnique*, *70*(4), 281-291. https://doi.org/10.1680/jgeot.18.P.023

Important note
To cite this publication, please use the final published version (if applicable).
Please check the document version above.

Ground response during offshore pile driving in a sandy slope

P. LAMENS*, A. ASKARINEJAD†, R.W. SLUIJSMANS‡ and A. FEDDEMA§

This paper presents an analysis of field measurements obtained during pile installation tests in a submerged sandy slope. The field test was performed in 2016 as part of the construction of a new sea lock in The Netherlands. Ground vibrations and excess pore pressures were to be limited in order to prevent damage to neighbouring locks and maintain slope stability. Geophones and piezometers were installed in the slope, at depth, and at various lateral distances from the pile axis. In the analysis, focus is placed on the installation of a tubular steel pile which was subjected to both vibratory and impact driving. An assessment is made of some factors, such as driving equipment and pile tip penetration depth, affecting both the magnitude of ground vibration and its spatial and temporal characteristics. A similar analysis is conducted of the pore pressure measurements, with particular attention paid to the part of driving carried out in a homogeneous sand layer. Measured vibrations and excess pore pressures are compared to established attenuation relationships and published data, respectively. An approach is suggested in which the test results and interpretation may be used in assessing the potential implications of excess pore pressure development in the sand layer for slope stability.

KEYWORDS: pile installation; vibratory pile driving; ground vibration; excess pore water pressure; slope stability

INTRODUCTION

In various civil, geotechnical and offshore applications piles or sheet piles are installed into fully saturated sands, for example into submerged slopes along harbour or port embankments, or during the foundation installation of offshore wind turbines.

A particular concern when examining fully saturated cohesionless soils affected by vibrations is the generation of excess pore water pressure, and potential liquefaction. Liquefaction of soils through cyclic loading is dominated in research by seismic studies. Other sources of vibrations, however, such as those induced by machines or wave loading, are also known to be able to trigger liquefaction.

Pile driving can be a source of ground vibrations, and, in the case of vibratory pile driving, (local) liquefaction is in fact the method by which the pile penetrates the soil medium. During both impact and vibratory pile driving, various stress waves cause ground motion. Compression waves propagate from from the pile toe over a spherical wavefront, whilst vertically oriented shear waves emanate from the pile shaft and expand over a conical surface (Attewell & Farmer, 1973). Some surface waves may also be induced by interacting body waves (Richart et al. (1970); Masoumi et al. (2007)). Characteristics and attenuation of ground vibrations induced by pile driving have been widely studied in the past (Jonker (1987); Massarsch et al. (2008)). Whenham, in her thesis (2011), examines the transfer of energy at the pile-soil interface, whilst Deckner (2013) treats the propagation of vibrations in the soil.

Several studies exist which examine pore pressures induced during pile driving in fine-grained soils. Among them Bjerrum & Johannessen (1960); Lo & Stermac (1965); Airhart et al. (1969); and Eigenbrod & Issigonis (1966). Many of these studies are motivated by the determination of pile set-up after installation by considering a disturbed zone, or zone of excess pore water pressure, as studied by Randolph and Wroth (1979). Measurements of excess pore pressure development during pile driving in *sand* are not as widely reported (Hwang et al., 2001). It is suspected that excess pore pressure development during driving in sand depends in part on the soil profile, i.e. on the confinement of the sand layer. A further warrant for investigation of pore pressures in sand, is that, in very loose sands, cyclic shear loading of soil may be responsible for considerable excess pore water pressure generation. In these types of sands, piling-induced ground vibration may cause (temporary) strength reduction of the soil. The link between vibrations and excess pore water pressure generation lies in the tendency of the soil to contract and undergo significant shear strain.

As part of the construction of a new sea lock in the North of the Netherlands, an extensive range of hollow tubular mooring piles and sheet piles are installed into submerged slopes. Meijers (2007) has noted that vibration measurements during pile driving may vary wildly in seemingly similar driving and soil conditions, and therefore the prediction of vibration amplitudes is often ambiguous. Insight is required into the potential significance of ground motion and excess pore water pressure generation during the pile drivings at the lock construction site. Therefore, several pile installation tests were carried out along the North Sea Canal, of which the resulting measurements are analysed and discussed. This paper exposes spatial and temporal trends of both vibrations and excess pore pressures measured during driving in a confined sand layer and suggests a holistic and practical approach for assessing the effect of the pile installation-induced soil response on slope stability.

DESCRIPTION OF TEST SITE AND MONITORING

A set of pile installation tests was carried out into a submerged slope of which the cross-section is shown in Fig. 1, indicating the location of the axis of installation of the piles with respect to a set of nine sensors. Geophones A01-A05 measured ground motion in terms of velocity and acceleration in three perpendicular directions. Data was measured at a frequency of 1 kHz, but logged at a mere 1 Hz. However, several traces of 1 kHz data are available. Transducers P01-P04 recorded pore water pressure at a frequency of 5 Hz during driving activity, with an accuracy of 0.1% Full Scale Output (FSO). These
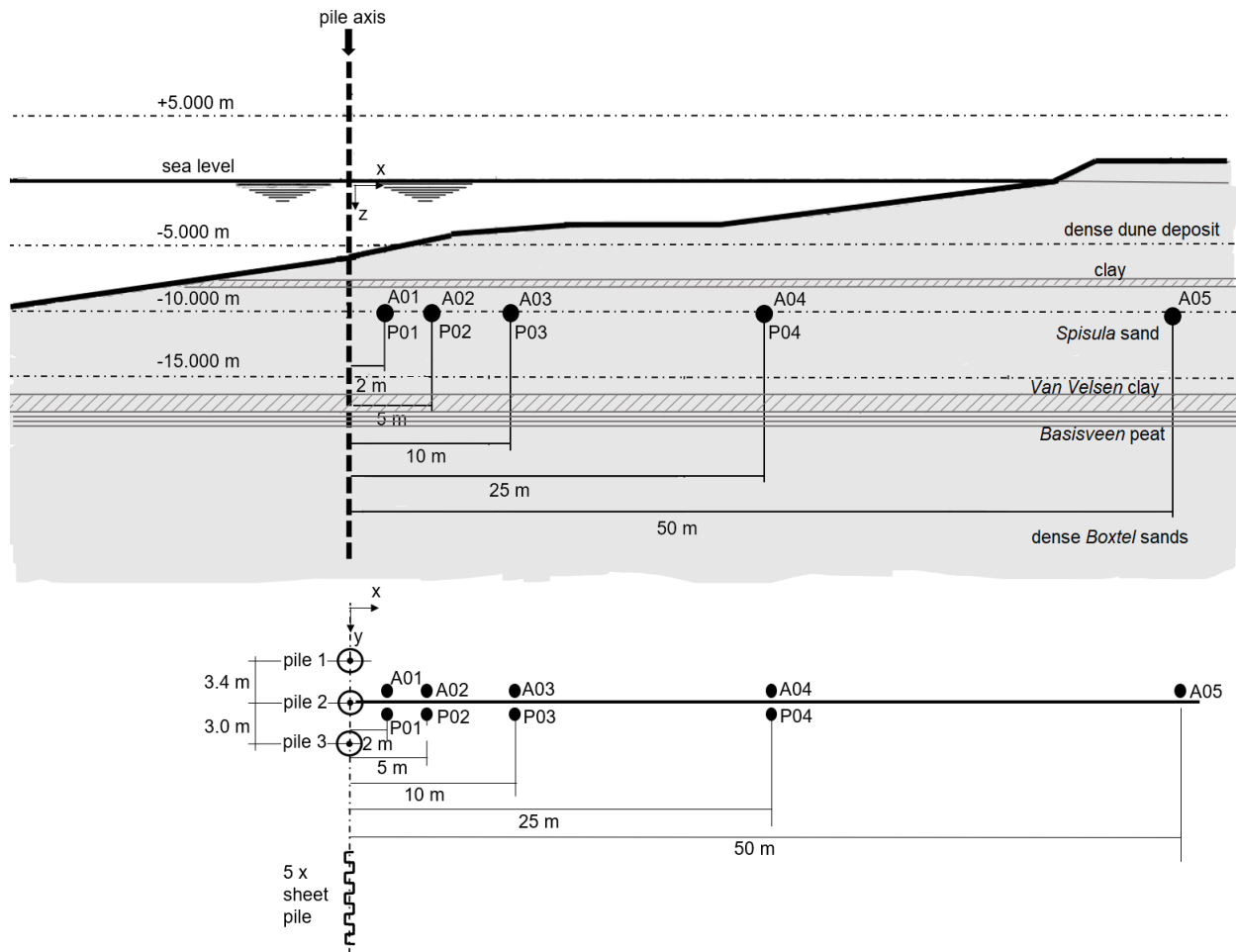

Fig. 1. Cross-section of test site and top view with monitoring equipment.

measurements were corrected for tidal fluctuations in water level. All sensors were placed at a depth of -10 m a.s.l.

As part of the pile installation tests, three hollow tubular steel piles and five steel sheet piles were installed, see the top view of the test location in Fig. 1. The focus of this study is placed on the installation of the first tubular steel pile (pile 1 in Fig. 1), given the 'undisturbed' conditions preceding its installation and lack of interruption during the driving process. Providing additional interest to this particular pile driving is the use of both a variable moment vibratory driver and a hydraulic impact hammer. Tab. 1 gives details of pile 1 and the driving equipment used to drive this pile. All vibratory driving activities on site involved a high-frequency (38 Hz) driving head, except for the driving of pile 3, which was carried out using a low-frequency (23 Hz) driving head.

The soils making up the slope consist predominantly of siliceous sand. A relatively thick sand layer containing *Spisula* shell fragments is confined by two thin clay layers. A typical profile of soils encountered at the test location is given in Tab. 2. A typical CPT profile is given in Fig. 2. From these CPT results a variation in density may be inferred within the Spisula sand layer: the deeper half of the layer (from -13 m a.s.l. to -15 m a.s.l.) has significantly higher values of cone resistance and is in a denser state than the upper half of the Spisula sand.

DESCRIPTION OF SPISULA SAND

Given the focus of the majority of this study on the first few metres of pile driving, and the potentially loose configuration of

Table 1. Pile driving parameters.

Pile type	Diameter, D	[mm]	1620
	Wall thickness	[mm]	25
Vibratory driving	Elevation at start	[m a.s.l.]	-7.3
	Max. power	[kW]	805
	Max. frequency	[Hz]	38
Impact driving	Elevation at start	[m a.s.l.]	-27.8
	Max. blow energy	[kJ]	120
	Max. blow rate	[blows/min]	44

Table 2. Typical soil stratigraphy at site.

From [m a.s.l]	To [m a.s.l]	Soil description
5	0	Loose, sandy fill
0	-8	Dense dune deposit
-8	-8.5	Clayey transition layer
-8.5	-16	Marine offshore *Spisula* sand
-16	-17.5	*Van Velsen* Clay
-18	-19	*Basisveen* peat
-19	-35	Dense *Boxtel* (fluvio-)aeolian sands

the sand between -8.5 and -13 m a.s.l. as deduced from several boreholes and CPTs carried out in and near the slope, the *Spisula* sand is investigated in particular detail. In geological terms, it is an offshore marine deposit belonging to the Bligh Bank Formation.
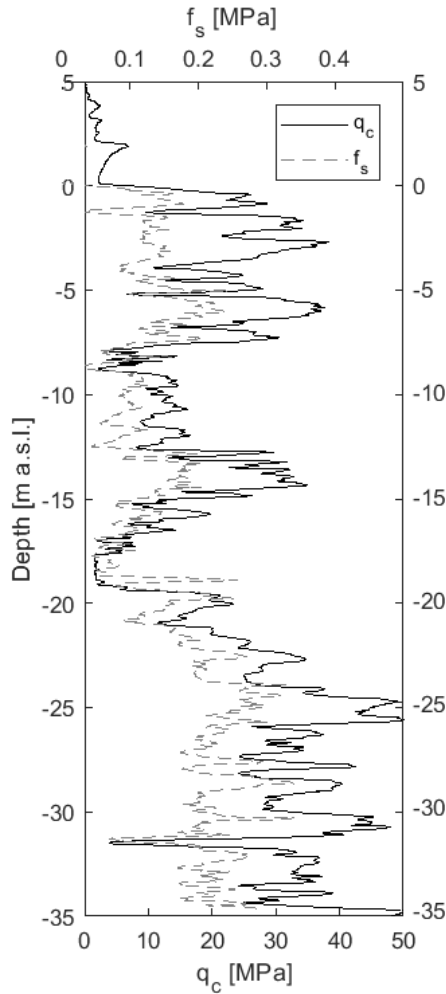
Fig. 2. A typical CPT performed on site showing cone resistance q_c and sleeve friction f_s with depth.

Borehole classification typifies the Spisula sand as a slightly silty, fine sand with thin layers of calcareous material and some small clay lenses. Sieving analyses of 100 samples indicate that the uppermost part of the Spisula sand consists of fine sand; $D_{50} = 130$ μm on average. Deeper down the material is slightly courser with an average D_{50} of 150 μm. The grain size distributions of the sand layer indicate that the material is quite uniform with a uniformity coefficient ranging from 1.4 to 2.2. The silt fraction of the samples varies between 4 and 12%, whilst the carbonate content lies between 8 and 20%. A typical particle size distribution curve is shown in Fig. 3.

Dry and saturated unit weights for the soil units found on site have been determined according to ISO/TS 17892-1&2 (2014) standards. For the Spisula sands typical values are 14.5 and 18.5 kN/m^3, respectively. The minimum and maximum densities of the sand are determined through the ASTM method (D4253) which was applied to 50 sand samples. The average minimum and maximum void ratios are 0.6 and 0.9, respectively. With an average value of 2.6 for the specific gravity, the in-situ relative density of the sand lies around 25%, which is classified as loose. The hydraulic conductivity of 18 samples of Spisula sand was determined according to ISO/TS 17892-11 (2004). The values of hydraulic conductivity are approximately $1 \cdot 10^{-5}$ m/s.

The mechanical properties of the Spisula sand were investigated using consolidated drained and undrained triaxial tests according to ISO/TS 17892-9 (2004). 40 samples of Spisula sand were subjected to monotonic triaxial testing.

The critical state friction angle of the sand was found to lie around 32°. Fig. 4 shows the response of a reconstituted sample densified to a relative density of 19%; anisotropically consolidated; and subjected to drained loading. The sample contracts throughout loading. Correspondingly, a reconstituted Spisula specimen, densified to a relative density of 25% and subjected to anisotropic consolidation followed by undrained loading, exhibits liquefaction behaviour, see Fig. 5.
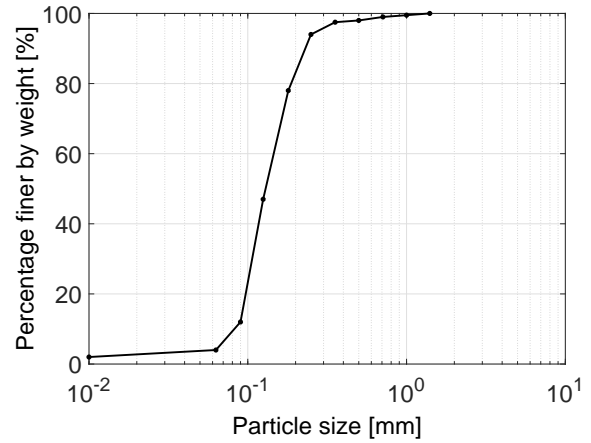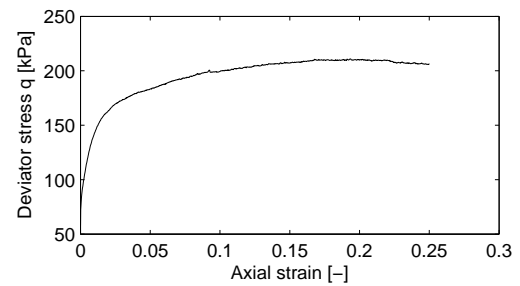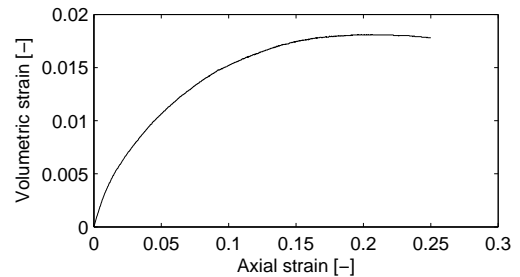

Fig. 3. Typical particle gradation curve of *Spisula* sand.

(a) Stress-strain response.

(b) Strain response.

Fig. 4. Behaviour of a reconstituted Spisula sand sample at 19% relative density during an anisotropically consolidated drained triaxial test.

MEASUREMENTS DURING PILE DRIVING

Measurements of ground acceleration and pore water pressure during the pile installation test are presented in this section. The entire duration of the driving of pile 1 is considered in order to be able to comment on general ground motion behaviour and pore water pressure in relation to pile penetration depth, soil layering, and driver operating pressure. The operating pressure, here, refers to pressure of the hydraulic fluid supplied to the
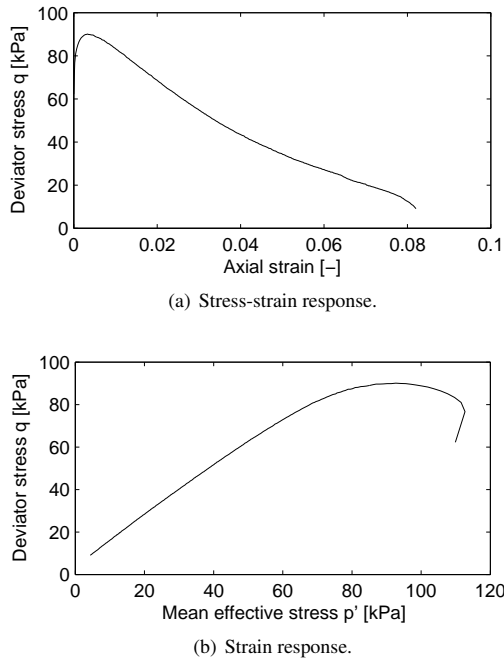
(a) Stress-strain response.

(b) Strain response.

Fig. 5. Behaviour of a reconstituted Spisula sand sample at 25% relative density during an anisotropically consolidated undrained triaxial test.

(a) Ground acceleration in time at various horizontal distances from the pile axis.

(b) Pile tip penetration depth and operating pressure in time.

(c) Ground acceleration at A01 versus operating pressure.

Fig. 6. Ground vibrations during vibratory driving of pile 1.

driver engine, and is therefore a measure of the input energy during driving.

Ground vibrations

The accelerations recorded at the five sensors during the vibratory driving of pile 1 are shown as a function of time in Fig. 6. The accelerations in *x*-direction are shown in this figure, which are generally slightly higher than those recorded in *y* and *z*-directions. The pile tip penetration depth and operating pressure in time are also given. The part of the driving carried out in the *Spisula* sand overlying the clay and peat layers is indicated, too.

Fig. 6(c) shows that a proportional relationship exists between the magnitude of ground vibrations and operating pressure. When the pile tip reaches the clay layer the operating pressure is reduced due to an increased ease of driving. The magnitude of induced ground acceleration, correspondingly, drops by a factor two at the sensor closest to the pile, A01. This supports observations made in previous investigations on the significance of source energy in determining vibration level. In fact, empirical relations based on the notion that potential or nominal energy of the pile driving equipment governs ground vibrations are widely used by practicing engineers (Jedele , 2005). However, the drop in acceleration amplitude may be more directly caused by a change in soil impedance. Massarsch and Fellenius (2008) find that ground vibration amplitudes are more directly tied to hammer properties, driving method, and soil properties than to potential or nominal energy of the driving equipment. Fig. 6(c) shows some outliers with peaking accelerations around 15 MPa of operating pressure, occurring during the transition from one soil layer to another around 15:59, see Figs. 6(a) and 6(b).
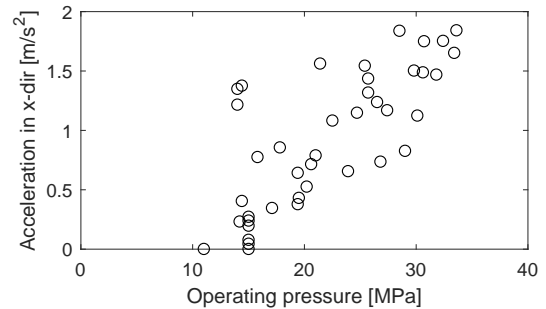
The vibrations generated during the subsequent impact driving of the pile to its final depth are visualised in Fig. 7. The maximum accelerations recorded by the sensors are a factor 2-3 greater than those recorded during vibratory driving. Considering the pile driving parameters for the two types of equipment as in Tab. 1, the energy input per second involved
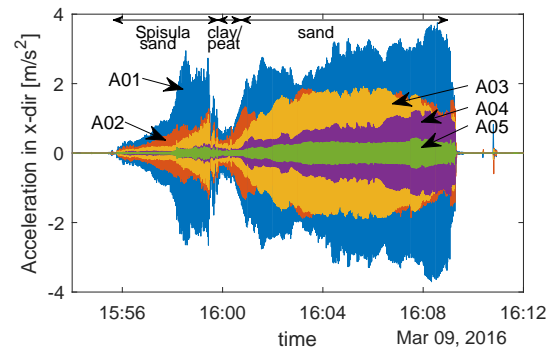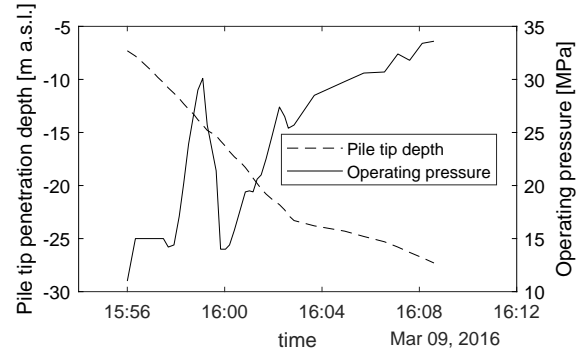
with each driving type may be calculated assuming a dwell time of one second for impact driving. The rate of energy transfer over such a small time scale is indeed greater for impact driving (120 kJ per second versus 21 kJ per second). Driving efficiency and soil conditions at various depths may also affect the rate of energy transfer.

The accelerations recorded during impact driving are independent of pile tip radial distance. Between -28 m a.s.l. and -34 m a.s.l. the soil conditions remain constant, see Tab. 2. Furthermore, the pile tip is far from the measurement points, so the stress waves affecting the sensors originate predominantly from the pile shaft.

Aside from amplitude, duration and frequency are important characteristics of a vibration signal. Traces of high-frequency ground motion measurements are presented in Figs. 8 to 10, showing the amplitude of ground motion in three perpendicular directions at the sensor closest to the pile, at 2.5D lateral distance. The figures also show frequency spectra, derived from the time domain using a Fourier transformation, giving the Power Spectral Density (PSD) of the measured velocities.
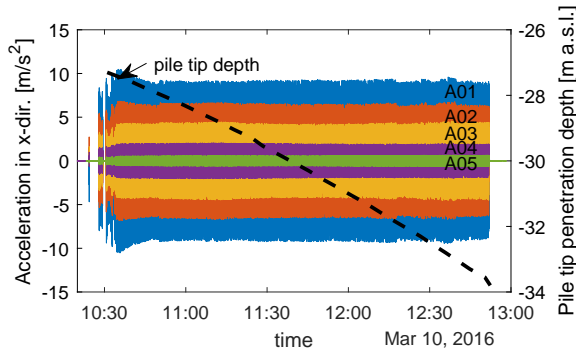
Fig. 7. Ground acceleration in time at various horizontal distances from the pile axis during impact driving.

Three situations are investigated (1) before driving (Fig. 8); (2) during vibratory driving (Fig. 9); and (3) during impact driving (Fig. 10). Fig. 8(b) suggests a dominant frequency of 'natural' ground motion at the site of around 5 Hz. These ground movements of the system in its 'natural' state could be caused by nearby construction activity, traffic, or waves, amongst others. During vibratory driving, the soil vibrates continuously and almost singularly at a frequency of 38 Hz; corresponding to the operating frequency of the vibratory driving head. Impact driving gives a very different soil response: the ground motion is transient, lasting for approximately 0.5 seconds as a result of the hammer blow. The range of frequencies at which the soil vibrates during impact driving is large, as shown in Fig. 10(b).
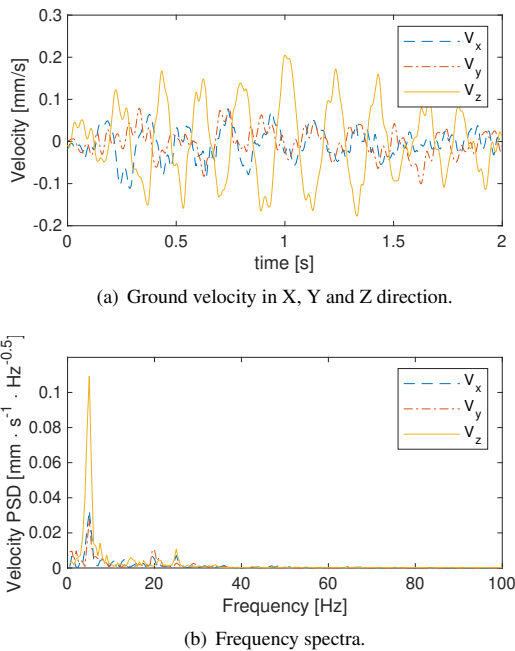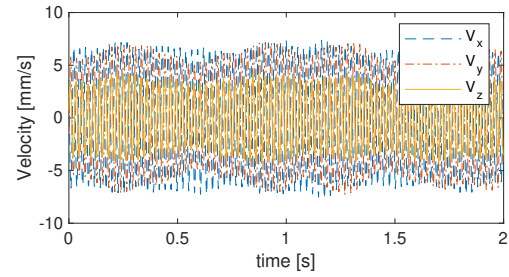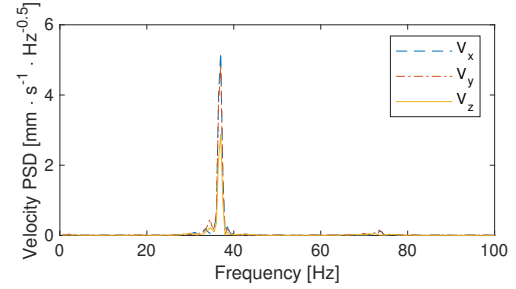

(a) Ground velocity in X, Y and Z direction.

(b) Frequency spectra.

Fig. 8. Ground motion before driving activity (09/03/2016 11:05:58) at sensor A01.

Pore water pressure
The pore water pressures measured during and after the driving of pile 1 are shown in Figs. 11 and 12, for vibratory and impact driving, respectively. Excess pore water pressures (EPPs) are derived from the pore water pressure measurements using an average value of hydrostatic pore pressure recorded before driving ensued. The figures indicate that whilst residual EPPs develop during vibratory driving, those generated during the
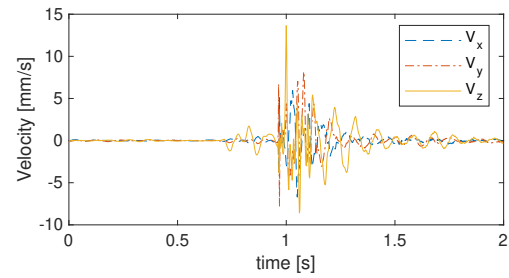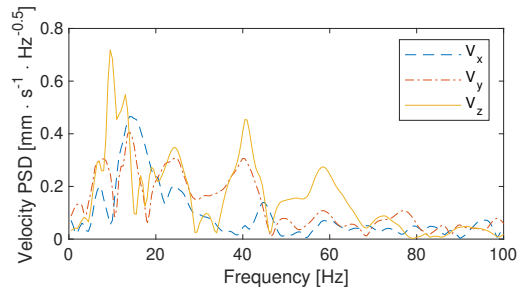

(a) Ground velocity in X, Y and Z direction.

(b) Frequency spectra.

Fig. 9. Ground motion during vibratory driving (09/03/2016 15:59:46) at sensor A01.

(a) Ground velocity in X, Y and Z direction.

(b) Frequency spectra.

Fig. 10. Ground motion during impact driving (10/03/2016 11:48:31) at sensor A01.

subsequent impact pile driving are transient. The maximum recorded EPPs at the sensor closest to the pile (A01) are similar for vibratory and impact driving. However, in general, much lower EPPs are generated during impact driving, with the bulk of the measurements showing values below 5 kPa.

Fig. 11 indicates that it takes roughly 10 min for 90% of the EPPs close to the pile to dissipate when vibratory driving ceases. It is not possible to comment on the degree of dissipation between each hammer blow, given the limited logging frequency of once every 30 s.
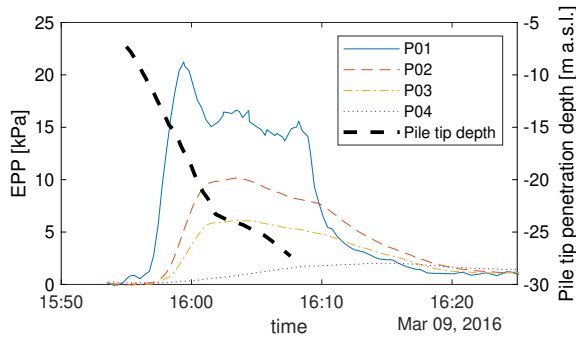
Fig. 11. Excess pore water pressure development during vibratory driving, measured at sensors P01-P04.
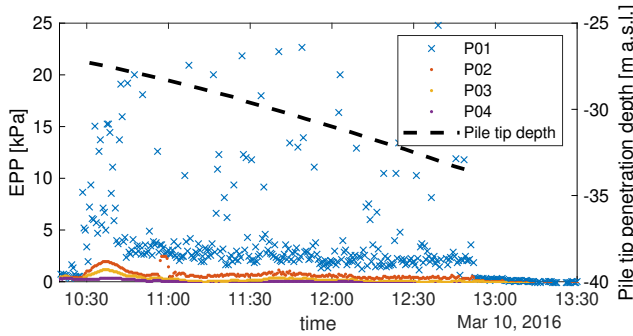

Fig. 12. Excess pore water pressure generation during impact driving, measured at sensors P01-P04.

RESPONSE OF THE SPISULA SAND
Ground vibrations
Effect of pile tip penetration depth

Besides operating pressure, it is of interest to investigate what effect the proximity of the pile tip to the sensor has on vibration amplitude. In order to do so, focus is put on the vibrations measured during vibratory driving in the *Spisula* sand layer only, which is confined by two clay layers as indicated in Tab. 2. Although the operating pressure is not constant during this first phase of driving (see Fig. 6), it is more suitable to draw conclusions about the influence of the advancing pile tip on ground motion when considering a soil stratum with approximately homogeneous characteristics. Fig. 6 indicates the measurement time considered in the following section, approximately lasting from 15:56 to 15:59.

The sensor closest to the pile (A01) shows the greatest difference in ground motion when the pile tip is above the sensor compared to when it is below, see Fig. 13. As the pile penetrates the soil, the dominant energy affecting the sensor is that from compression or P-waves, emanating from the pile tip. When the pile reaches the sensor and continues below, shear or S-waves emanating from the shaft contribute to ground motion. Therefore, the expectation from theory is that the vibrations amplitudes reach a constant level (Richart et al. (1970); Attewell & Farmer (1973)), or even decrease due to partial liquefaction around the pile, limiting the propagation of shear waves. Fig. 13, however, indicates somewhat increasing vibration amplitudes even after the pile tip has passed the sensor level. This could be explained by the increasing density of the Spisula sand as the pile moves downwards, leading to a greater energy input required for pile penetration. Fig. 2 shows the increasing cone resistance within the Spisula sand layer and Fig. 6(b) shows the increase in operating pressure of the vibratory driving machine, until it drops upon reaching
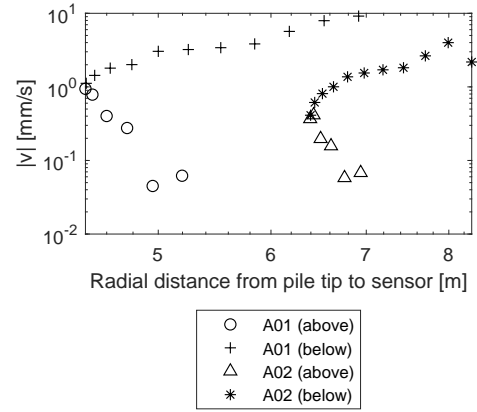

Fig. 13. Absolute velocity versus radial distance between the pile tip and the sensor, measured during vibratory driving of pile 1 in the Spisula sand, at sensors A01 and A02. *above* **and** *below* **indicate the position of the pile tip relative to the sensor.**

the clay layer. The excess pore pressures recorded at the sensor closest to the pile do not show high enough values to indicate liquefaction occurring at this distance from the pile, see Fig. 11. Therefore, the increment in operating pressure is a plausible explanation for the continued increase in ground velocity amplitude.

Attenuation characteristics

Plotting the absolute ground velocity measured at various time instances, or pile tip penetration depths, with distance from the source, results in Fig. 14 for the vibratory driving of pile 1. The pile tip is considered the dominant source of stress waves.

During vibratory driving, vibrations generally grow in amplitude as the pile descends into the sand, but the attenuation characteristic remains relatively similar throughout. This attenuation characteristic represents a combination of geometrical and material damping. Bornitz (1931) formulated an attenuation relation to describe these two forms of damping:

$$A_2 = A_1 \left(\frac{r_1}{r_2}\right)^n e^{-\alpha(\frac{r_2}{D} - \frac{r_1}{D})} \tag{1}$$

with A_2 and A_1 the desired and known vibration amplitude, respectively; r_1 and r_2 the corresponding radial distances from the source, normalized to pile diameter D; n the geometrical damping coefficient; and α the material damping coefficient. The values for A_1 and r_1 are based on assumed knowledge of the magnitude of vibration at the pile shaft - soil interface. Therefore, r_1 is taken as a very small distance e.g. 10 mm, whilst A_1 is determined from the shear stress amplitude at the pile-soil interface, following Massarsch and Fellenius (2008). Meijers (2007) suggests that the soil at the pile-soil interface is in a state of failure during pile installation, and therefore the maximum shear stress τ that can be transferred at the interface is that at yielding

$$\tau_{yield} = \sigma'_h \tan(\delta) = K\sigma'_v \tan(\delta) \tag{2}$$

with δ the friction angle between the pile and the soil. The coefficient of lateral earth pressure K is assumed to be neutral in Meijer's (2007) model, but it is expected that it will change throughout the vibratory driving process (Lehane et al. , 1993). The shear stress amplitude at the pile-soil interface may be further reduced by excess pore water pressure generation, up until a point of 'liquefied' or 'residual' strength, see e.g. (Holeyman et al., 1996).
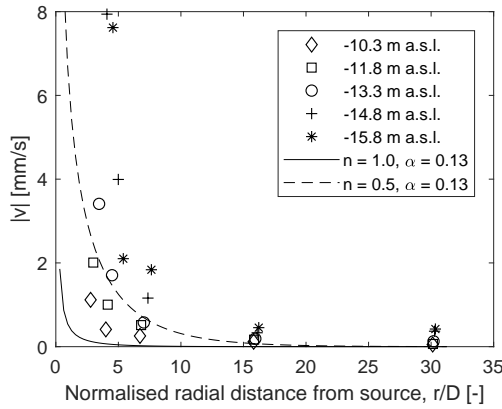
Fig. 14. Absolute velocity versus normalised radial distance from the pile tip, measured during driving in the Spisula sand layer, at various pile tip penetration depths.
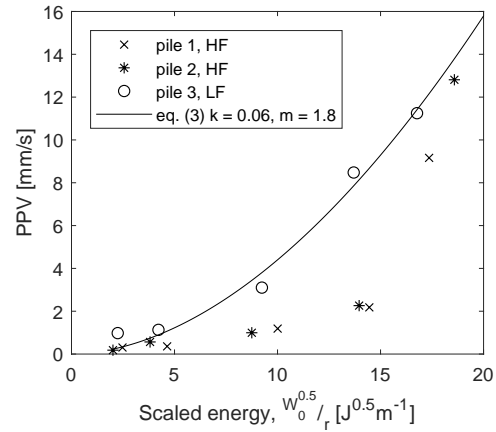

Fig. 15. Relationship between peak particle velocities measured during various driving activities and the radial distance from the pile tip, taking into account source energy. *HF* and *LF* refer to high-frequency and low-frequency vibratory driving, respectively.

In literature, often the use of $n = 1.0$ is recommended for pile driving (Kim & Lee, 2000). However, because the use of $n = 1.0$ represents the geometrical attenuation of shear waves propagating with a conical wave front, the use of this value for n is more suitable when examining pile driving deeper down, when the significance of the pile tip in stress wave production is smaller. Equation 1 is applied to ground velocity amplitudes measured during driving. Fig. 14 shows the overestimation of attenuation as when using $n = 1.0$. Using a geometrical attenuation coefficient of 0.5 results in an average material damping coefficient α of 0.13, which is a value for sand in reasonable correspondence with literature (Richart et al. (1970); Das (1983)). The use of $n = 0.5$ in combination with this level of material damping gives a better match with the data in Fig. 14.

In addition to distinguishing between geometrical and material damping in examining vibration attenuation, Attewell et al. (1973) (1992) suggest taking into account the effect of driving energy using the following relation

$$PPV = k \left(\frac{\sqrt{W_0}}{r} \right)^m \qquad (3)$$

where PPV is the peak particle velocity measured at the site, expressed in mm/s; W_0 is the source energy in joules; r is the radial distance from the source in metres; k represents the intercept value of vibration amplitude; and m is a parameter accounting for site-specific attenuation. The source energy may be computed from the power input during vibratory driving or from the energy involved with a single hammer blow during impact driving (Head & Jardine, 1992). Often used values for m lie between 1.0 and 2.0 (Whenham (2011); Massarsch et al. (2008)). Attewell et al. (1992) suggest a conservative value for both k and m of 1.0 for use in design.

The pile installation tests at the focus of this study involved the vibratory driving of (sheet)piles using various driving equipment: high-frequency (38 Hz) driving for pile 1 and pile 2 and low-frequency (23 Hz) driving for pile 3. It is of interest to compare the maximum amplitude of the vibrations generated by each installation versus the radial distance to the pile tip, taking into account driving energy, which differs per driving technique. Fig. 15 illustrates this for the three different drivings. For each driving the considered time instant is that at which absolute velocities are greatest at sensor A01 during driving in the Spisula sand layer only. The input energy W_0 is determined from the operating pressure at this time instant. The maximum operating pressure is taken equal to the maximum power input,

and a linear relationship is assumed between the two. It is clear from Fig. 15 that low-frequency vibratory driving induces relatively high vibrations, even when discounting for the low input energy relative to the input energy as a result of high-frequency driving. When applying equation 3 to the PPVs caused by the driving of pile 3, coefficients $k = 0.06$ and $m = 1.8$ give a least-square error fit. The level of attenuation for this low-frequency driving activity is within the expected range of $n = 1.0 - 2.0$, whilst the high-frequency driving of piles 1 and 3 is accompanied by higher levels of attenuation.

Ground motion

In order to evaluate the characteristics of vibratory piling induced vibration, the variation in ground motion in three orthogonal planes, measured during the driving of pile 1, is plotted in Fig. 16, at various horizontal distances from the pile driving axis. The ground motion shows mostly equal horizontal and vertical components with some elliptical motion, suggesting that the motion is not solely the result of vertically polarised shear waves. Masoumi (2007) indicates that in a zone near the surface, Rayleigh waves also play a role, especially in the far field, when body waves have mostly attenuated.

Zone of densification

A zone of densification, or plastic behaviour, around a pile may be deduced from acceleration, velocity or strain criteria, found in various literature (Barkan (1962); (Selig , 1963)). Considering the latter criterion of strain, Massarsch and Fellenius (2002) as well as Bement and Selby (1997) expect densification above 0.001% strain. Dobry et al. (2015) give a threshold cyclic shear strain for volume change and pore pressure increase in sands of 0.01%.

Typical strain levels during the vibratory driving of pile 1 may be derived from the high-frequency measurements in Fig. 16 and by assuming a linear-elastic relationship between strain and ground velocity: $\gamma = v/c_s$, with c_s the shear wave velocity (Massarsch, 2004). Fig. 17 shows the resulting strain-distance relationship from which a radial zone of densification around the pile may be interpreted: approximately 6D, in this case. Of course, a great assumption here lies in considering the ground motion to correspond to shear strain, even though in reality it may show a combination of both shear and volumetric strain, depending on the type of stress waves imposed upon the soil.
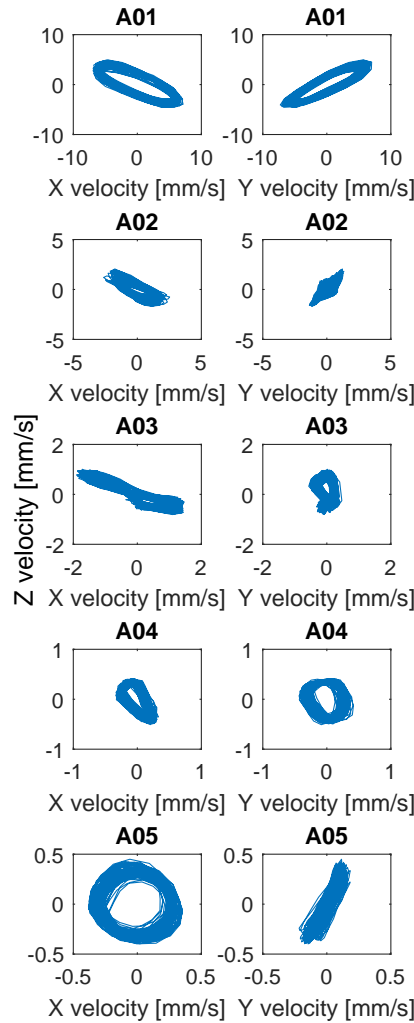
Fig. 16. Ground motion in terms of X, Y and Z velocities during two seconds of vibration measurements during vibratory driving of pile 1 around 15:59:00 on 09/03/2016, at a pile tip penetration depth of -15.5 m a.s.l. Data is sampled at 1 kHz.
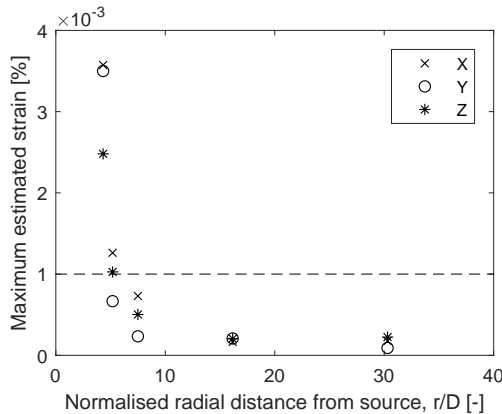

Fig. 17. Determination of plastic zone around a pile based on a threshold shear strain level of 0.001%. Strain levels are estimated using Fig. 16.
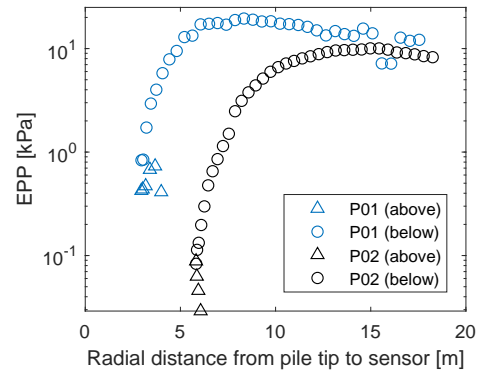
Fig. 18. EPP versus radial distance between the pile tip and the sensor, measured during the vibratory driving of pile 1. *(above)* and *(below)* indicate the position of the pile tip relative to the sensor.

Pore water pressure
Effect of pile tip penetration depth

The excess pore water pressure development in the sandy layer whilst the pile is penetrating this layer is also of interest. The EPP as a function of radial distance between the pile tip and the sensor, for the two sensors closest to the pile, is shown in Fig. 18. EPPs start to accumulate rapidly as soon as the pile tip passes the sensor level. This is in line with what is expected from theory: residual excess pore water pressure accumulates due to cyclic shear loading, caused by shear waves emanating from the pile shaft.

Decay with distance from pile

Maximum EPPs are compared to data from literature in Fig. 19. Data presented in blue shows values measured in clay, whilst black indicates sandy soil. To enable comparison, the EPPs have been normalized with effective stress level to give the relative excess pore water r_u. The horizontal distance x from the pile has been normalized with pile diameter D. Using maximum EPP values may appear conservative for design purposes, since these peaks in EPP generally do not occur simultaneously at the various x distances from the pile, due to gradual radial drainage. However, the use of maximum EPPs is often encountered in literature and allows the incorporation of measurements from interrupted pile drivings.

Fig. 19 indicates that, within the range of x/D considered, the maximum EPPs measured in sand during the pile installation tests are generally lower than values reported in clay. Hwang et al. (2001) report values measured in sand that are as high as ones found in clay, which could be attributable to the more extreme confinement of the sand layer in the study of Hwang et al.: 4 m of sand confined by two thick clay layers. The time extent for which EPPs exist in the soil is not considered in Fig. 19. An average exponential fit to the data from literature, indicated with a dashed line in Fig. 19, gives a relationship between the maximum relative excess pore pressure and the scaled horizontal distance from the pile:

$$r_{u,max} = 2.6e^{-0.22\frac{x}{D}} \qquad (4)$$

Dissipation of excess pore water pressure

From Fig. 11 a time shift may be observed between the occurrence of peak excess pore pressure at the different sensors. This suggests that a certain level of radial drainage is occurring. Randolph and Wroth (1979) claim most excess pore
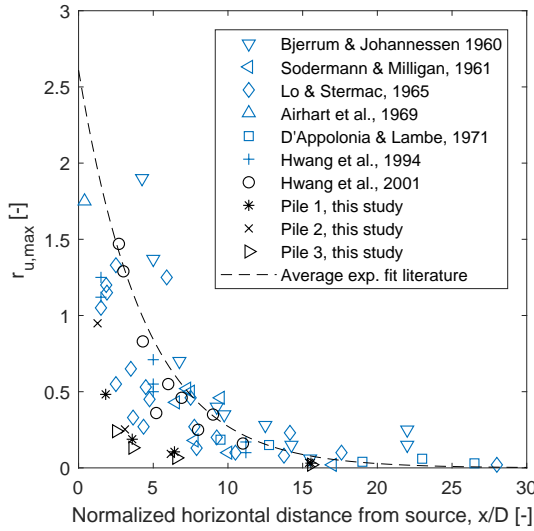
Fig. 19. Literature review of maximum relative excess pore water pressure as a function of the normalized horizontal distance from the source of vibration. Values reported in blue were found in clay; values in black were found in sand.

water drainage after driving occurs radially, since studies have indicated that the major pore pressure gradients around a driven pile are radial (Bjerrum & Johannessen (1960); Lo & Stermac (1965)).

The degree of drainage *during* driving may be interpreted by comparing the characteristic drainage time of a soil to driving-related time periods. The characteristic drainage time of a soil T_{char} may be determined from the drainage path length L and the coefficient of consolidation c_v

$$T_{char} = \frac{L^2}{c_v} \tag{5}$$

The relevant drainage path length, in this case, is the equivalent diameter of a solid pile, amounting to approximately 0.4 m in the case of pile 1 (Randolph , 2003). A consolidation coefficient of the Spisula sand of 0.002 m^2/s, estimated from the measured hydraulic conductivity of $1 \cdot 10^{-5}$ m/s, and a time factor T_{90} for consolidation around a driven pile equal to 10, leads to a 90% EPP dissipation time $t_{90} = T_{90} D_{eq}^2 / c_v$ of roughly 13 min. This is consistent with the 90% decay time of residual EPPs close to the pile as deduced from Fig. 11.

Considering the different mechanisms of EPP build-up: a single loading cycle during vibratory driving lasts for $1/38$ Hz or 0.026 s, whilst the total duration of driving may be 5-10 min. It becomes clear that instantaneous excess pore pressure generation, generated within a single loading period, occurs under practically undrained conditions. However, the total duration of loading may be of a similar order of magnitude as the characteristic drainage time. Therefore, residual excess pore pressures may accumulate in a partially drained environment.

IMPLICATIONS FOR SLOPE STABILITY
The stability of a slope may be negatively affected by pile driving in two ways: (1) through dynamic or inertia-related effects and (2) through excess pore pressure development, diminishing effective stress and, correspondingly, the mobilisable shear strength in the soil. When considering vibratory pile driving in a sandy slope, the former effect is of inferior importance to the latter (Meijers, 2007). The residual excess pore water pressures which accumulate during vibratory

pile driving are a result of cyclic loading. Cyclic liquefaction criteria may be used to determine the susceptibility of sand in slopes to cyclic liquefaction (e.g. Castro & Poulos (1977); Vaid & Chern (1985)). However, the full-scale test of this study has shown that excess pore water pressure zones develop locally and that pore water migrates in time. In order to take these effects into account when evaluating the static safety of a slope, whether it be through limit equilibrium or finite element methods, the effect of excess pore pressure on mobilisable shear strength throughout the slope must be accounted for *in time*. Fig. 20 outlines a slope stability assessment method. It advocates assessing the pre-pile installation stability of the slope first. EPP development in liquefiable layer(s) in time due to pile driving is modelled at various distances from the pile installation axis. This may be done numerically, or by using an empirical relation for EPP decay with distance for a specific site, such as equation 4. Next, the EPPs are inputted directly into the slope stability analysis software or are implemented through reduction in mobilisable shear strength. In this way the stability of the slope may be determined taking into account pile installation effects. Effects of the physical presence of the pile; dynamic effects; void redistribution; or three-dimensional (radial) drainage form potential additions to this method.

CONCLUSION
From the preceding analysis it becomes clear that vibratory and impact pile driving induce different ground vibrations and excess pore pressures. The continuous and high-frequency loading the soil experiences during vibratory driving leads to the development of residual excess pore water pressure, as well as ground motion which is generally of smaller amplitude than that caused by a hammer blow.

The measurements indicate that input energy and driving frequency affect vibration amplitudes. This input energy may correspond to the potential or nominal energy of the driving equipment, but may be further impacted by pile and soil impedance. Pile impedance, however, is not expected to affect ground vibrations in the dynamic field at some distance from the pile. Low-frequency driving induces greater vibrations than high-frequency driving, which corresponds to expectations.

Pile tip penetration depth, too, has an effect on vibration attenuation characteristics. Whilst driving in the Spisula sand layer, the soil appears to not solely be affected by vertically polarised shear waves emanating from the pile shaft. Both the geometric attenuation deduced from measurements and the ground motion records suggest otherwise. This could be explained by the early stage of driving, or by stress wave interaction as a result of the layered soil system. Dowding (1996), Svinkin (2008) and, more recently, Deckner et al. (2017) note the importance of pile driving-induced Rayleigh waves. Therefore, besides driving energy and frequency, the type of induced stress waves and their interaction dominate the ground motion response.

The excess pore pressure development in time may also be affected by the layering of the soil system. The confinement of the sand layer between two clayers increases the potential for residual excess pore pressure. Excess pore pressures in the soil surrounding the pile appear to be generated primarily when the pile tip has passed the sensor level, indicating the significance of shear waves emanating from the pile shaft during vibratory driving in the build-up of residual excess pore pressures.

The exact link between ground motion and excess pore pressures, however, is difficult to make. It is not possible to distinguish between compression and shear waves from the acceleration records presented in this study, as the logging frequency is not high enough. The exact loading cycle, as
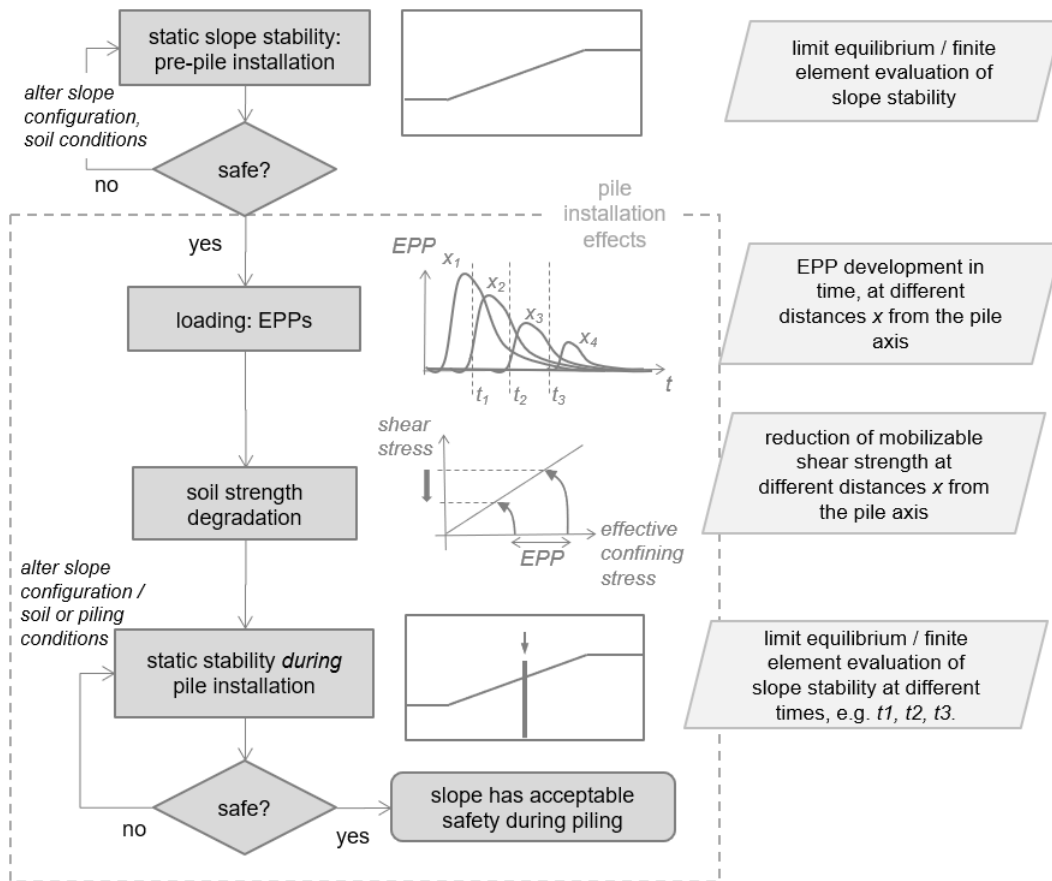
Fig. 20. Conceptual framework for assessing slope stability as a result of excess pore water pressure generation during vibratory pile driving.

well as the instantaneous excess pore pressure generated as a consequence, are not captured in this study.

On the other hand, it is possible to comment on the zone of potentially significant plastic behaviour, or densification, from vibration measurements. This zone corresponds to a zone of excess pore pressure generation as a result of driving. However, pore pressure records indicate that in sand, with a relatively high permeability, interim radial drainage is an important phenomenon to consider when looking at vibratory pile driving. Unlike in most earthquake analyses, the situation under consideration may not be fully undrained. This has implications for the stability of a slope, which may alter over time as pore water migrates.

NOTATION

D pile diameter

A	vibration amplitude
r	radial distance
n	geometrical damping coefficient
α	material damping coefficient
τ_{yield}	shear stress at yielding
σ'_v	vertical effective stress
σ'_h	horizontal effective stress
δ	friction angle between pile and soil
K	coefficient of lateral earth pressure
PPV	peak particle velocity
k	intercept value of vibration amplitude
W_0	source energy
m	attenuation parameter
$r_{u,max}$	maximum relative excess pore pressure
x	horizontal distance from pile
T_{char}	characteristic drainage time
L	drainage path length
c_v	vertical consolidation coefficient

REFERENCES

Airhart, T.P., Coyle, H.M., Hirsch, T.J. & Buchanan, S.J. (1969). Pile-soil system response in cohesive soil. *Performance of Deep Foundations (STP 444)*, 264-294.

Attewell, P.B. & Farmer, I.W. (1973). Attenuation of ground vibrations from pile driving. *Ground Engineering* 6, No.4, 26-29.

Attewell, P.B., Selby, A.R. & O'Donnell, L. (1992). Estimation of ground vibration from driven piling based on statistical analyses of recorded data. *Geotech. Geol. Engrg.* 10, No. 1, 41-59.

Barkan, D. (1962). *Dynamics of Bases and Foundations*. New York: McGraw-Hill Book Company.

Bement, R.A.P. & Selby, A.R. (1997). Compaction of granular soil by uniform vibration equivalent to vibrodriving of piles. *Geotech. Geol. Eng.* 19, No. 2, 115-126.

Bjerrum, L. & Johannessen, I.J. (1960). Pore pressure resulting from driving piles in soft clay. *Proc., Conf. on Pore Pressure and Suction*

in Soils, Butterworths, Sydney, 108-111.

Bornitz, G. (1931). *Expansion of heavy drilling producing ground motion in the deep.* Berlin: J. Springer.

Castro, G. & Poulos, S.J. (1977). Factors affecting liquefaction and cyclic mobility. *J. Geotech. Geoenviron. Eng.* 103, No. 6.

D'Appolonia, D.J. & Lambe, T.W. (1971). Performance of four foundations on end-bearing piles. *J. Soil Mech. Found. Div.*, 97, No. 1, 77-93.

Das, B.M. (1983). *Fundamentals of soil dynamics.*

Deckner, F. (2013) *Ground vibrations due to pile and sheet pile driving: influencing factors, predictions and measurements.* Doctoral dissertation, KTH Royal Institute of Technology, Sweden.

Deckner, F., Viking, K. & Hintze, S. (2017). Wave patterns in the ground: case studies related to vibratory sheet pile driving. *Geotech. Geol. Engrg.* 35, No. 6, 2863-2878.

Dobry, R., & Abdoun, T. (2015). Cyclic shear strain needed for liquefaction triggering and assessment of overburden pressure factor Kσ. *J. Geotech. Geoenviron. Eng.*, 141, No. 11.

Dowding, C.H. (1996). *Construction vibrations.* Vol. 81. Upper Saddle River, NJ: Prentice Hall.

Eigenbrod, K.D. & Issigonis, T. (1966). Pore-water pressure in soft to firm clay during driving of piles into underlying dense sand. *Can. Geotech. J* 33, 209-218.

Head, J.M. & Jardine, F.M. (1992). Ground-borne vibrations arising from piling. *CIRIA Tech. Note*, 142.

Holeyman, A.E., Legrand, C., & Rompaey, D. van (1996). A method to predict the driveability of vibratory piles. *Proc. 5th Int. Conf. Appl. Stress-Wave Theory to Piles, Orlando*, 1101-1112.

Hwang, J.H., Lee, C.C., Fang, J.S. & Chang, J.Z. (1994). Behavior of frictional driven pile in underconsolidated clay. *1st Int. Symp. Struct. and Found., Hangchow.*

Hwang, J.H., Liang, N. & Chen, C.H. (2001). Ground response during pile driving. *J. Geotech. Geoenviron. Engrg.* 127, No. 11, 939-949.

International Organization for Standardization (2014). Geotechnical investigation and testing – Laboratory testing of soil – Part 1: Determination of water content & Part 2: Determination of bulk density (ISO/TS 17892-1&2:2014(E)).

International Organization for Standardization (2004) Geotechnical investigation and testing – Laboratory testing of soil – Part 9: Consolidated triaxial compression tests on water saturated soil (ISO/TS 17892-9:2004(E)).

International Organization for Standardization (2004) Geotechnical investigation and testing – Laboratory testing of soil – Part 11: Determination of permeability by constant and falling head (ISO/TS 17892-11:2004(E)).

Jedele, L.P. (2005). Energy-Attenuation Relationships from Vibrations Revisited. *GeoFrontiers 2005. Soil Dynamics Symposium in Honor of Professor Richard D. Woods, Austin, Texas.* American Society of Civil Engineers, Geotechnical Special Publication 134, 1467-1480.

Jonker, G. (1987). Vibratory pile driving hammers for pile installations and soil improvement projects. *Offshore Tech. Conf., Houston, Texas.*

Kim, D.S. & Lee, J.S. (2000). Propagation and attenuation characteristics of various ground vibrations. *Soil Dyn. Earthq. Eng.* 15, No. 2, 121-143.

Lehane, B.M., Jardine, R.J., Bond, A.J. & Frank, R. (1993). Mechanisms of shaft friction in sand from instrumented pile tests. *J. Geotech. Engrg.* 119, No. 1, 19-35.

Lo, K.Y. & Stermac, A.G. (1965). Induced pore pressure during pile driving operations. *Proc., 6th Int. Conf. Soil Mech. Found. Engrg., Toronto,* 2, 285.

Masoumi, H.R., Degrande, G. & Lombaert, G. (2007). Prediction of free field vibrations due to pile driving using a dynamic soil–structure interaction formulation. *Soil Dyn. Earthq. Eng.* 27, No. 2, 126-143.

Massarsch, K.R. (2004). Vibrations caused by pile driving. *Deep Foundation Institute Magazine, Summer and Fall Featured Articles*, Hawthorne.

Massarsch, K.R. & Fellenius, B.H. (2002). Vibratory compaction of coarse-grained soil. *Can. Geotech. J* 39, No. 3, 695-709.

Massarsch, K.R., Fellenius, B.H. & Bengt, H. (2008) Ground vibrations induced by impact pile driving. *Int. Conf. Case Hist. Geotech. Engrg., Missouri.*

Meijers, P. (2007). *Settlement during vibratory sheet piling.*

Randolph, M.F. & Wroth, C.P. (1979). An analytical solution for the consolidation around a driven pile. *Int. J. Numer. Anal. Methods Geomech.* 3, No.3, 217-229.

Randolph, M.F. (2003). Science and empiricism in pile foundation design. *Géotechnique* 53, No. 10, 847-876.

Richart, F.E., Hall, J.R. & Woods, R.D. (1970). *Vibration of soils and foundations.* Englewood Cliffs, NJ: Prentice-Hall.

Selig, E.T. (1963). *in Proc., 2nd Pan-Am. Conf. Soil Mech. Found. Eng.*, Vol. 1, 129-144.

Soderman, L.G. & Milligan, V. (1961). Capacity of friction piles in varved clay increased by electro-osmosis. *Proc., 5th Int. Conf. Soil Mech. Found. Engrg., Dunod, Paris*, 1, 319-326.

Svinkin, M.R. (2008). Soil and structure vibrations from construction and industrial sources. *Int. Conf. Case Hist. Geotech. Engrg. Arlington, Virginia.*

Vaid, Y.P. & Chern, J.C. (1985). Cyclic and monotonic undrained response of saturated sands. *Advances in the art of testing soils under cyclic conditions.*, ASCE, 120-147.

Whenham, V. (2011) *Power transfer and vibrator-pile-soil interactions within the framework of vibratory pile driving.* Doctoral dissertation, University of Louvain, Belgium.

Figure2
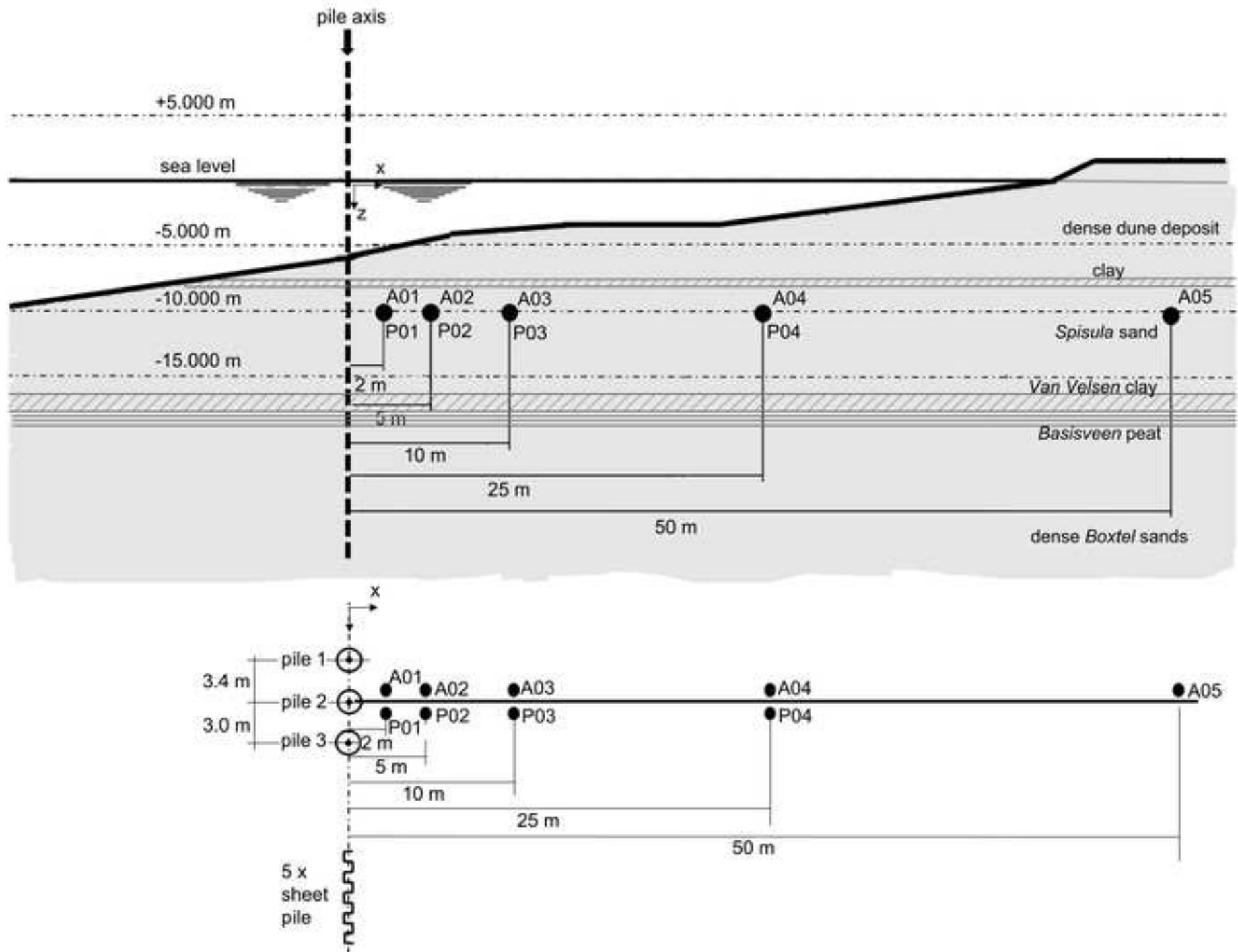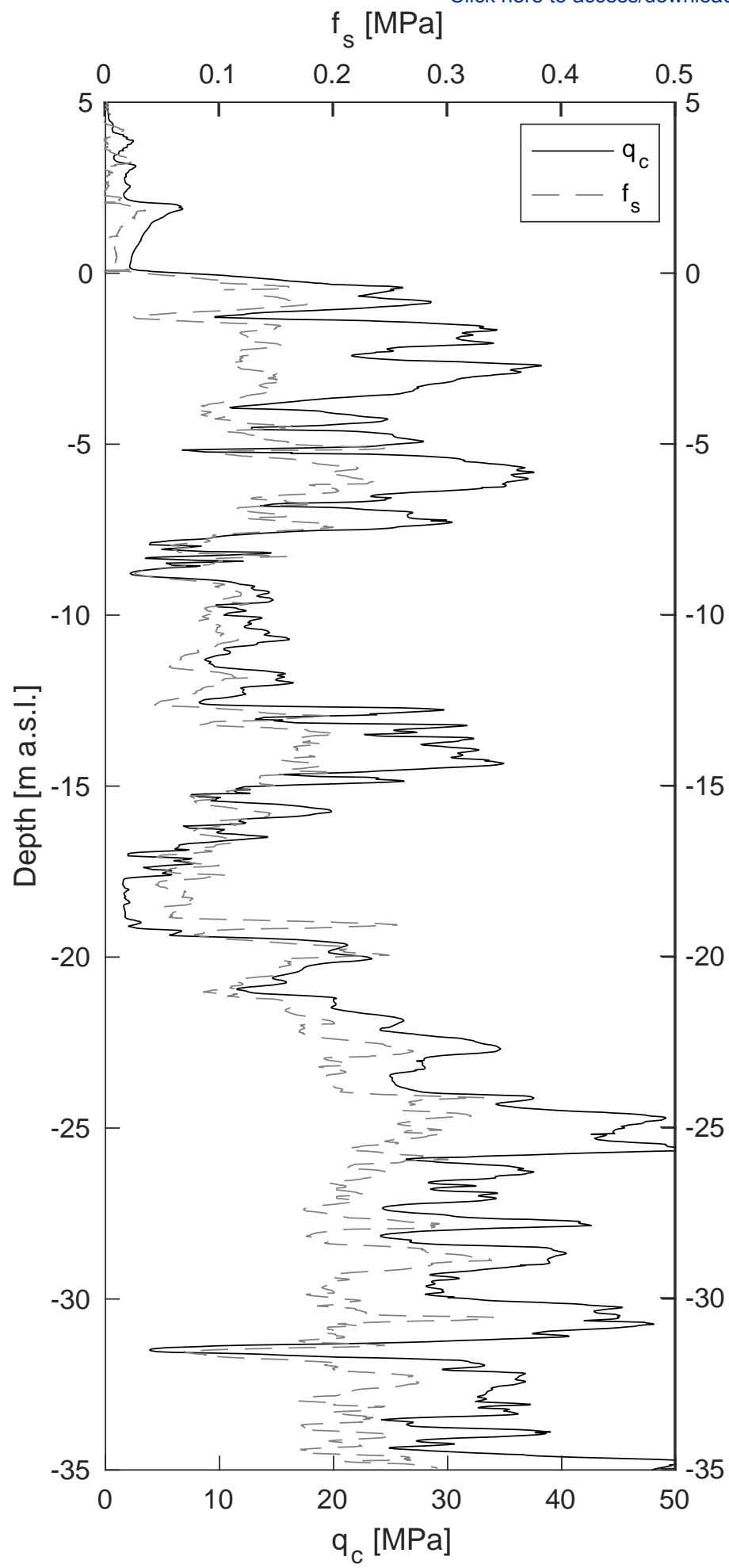
Figure3

Figure7

Figure11

Figure12

Figure13

Figure14

Figure 14

Figure15

Figure16

Figure17

Figure18

Figure19

Figure20

Table 1. Pile driving parameters.

Pile type	Diameter, D	[mm]	1620
	Wall thickness	[mm]	25
Vibratory driving	Elevation at start	[m a.s.l.]	-7.3
	Max. power	[kW]	805
	Max. frequency	[Hz]	38
Impact driving	Elevation at start	[m a.s.l.]	-27.8
	Max. blow energy	[kJ]	120
	Max. blow rate	[blows/min]	44

Table 2. Typical soil stratigraphy at site.

From [m a.s.l]	To [m a.s.l]	Soil description
5	0	Loose, sandy fill
0	-8	Dense dune deposit
-8	-8.5	Clayey transition layer
-8.5	-16	Marine offshore *Spisula* sand
-16	-17.5	*Van Velsen* Clay
-18	-19	*Basisveen* peat
-19	-35	Dense *Boxtel* (fluvio-)aeolian sands

Dr. Amin Askarinejad
Assistant Prof. of experimental soil mechanics
Faculty of Civil Engineering and Geosciences,
TU Delft, the Netherlands,
Formerly at IGT, ETH Zurich, Switzerland

Address: Stevinweg 1 / PO-box 5048
2628 CN Delft / 2600 GA Delft
The Netherlands

Phone: +31 (0) 15 2783326
E-mail: A.Askarinejad@tudelft.nl
http://www.citg.tudelft.nl/aaskarinejad

Delft, 02-03-2019

Dear *Géotechnique* editor,

We wish to submit the final version of the manuscript entitled "Ground response during offshore pile driving in a sandy slope" for publication by Géotechnique.

We would like to thank the Journal assessor and the reviewers for their helpful feedback to the previous revisions. A list of notations has been added to this final version of the paper. Moreover, the figures have been updated according to the guideline of the journal.

Please address all correspondence concerning this article to me at A.Askarinejad@tudelft.nl.

Thank you for your consideration.

Sincerely,

Dr. Amin Askarinejad